

Spectral AB Simulations for Coastal and Ocean Engineering Applications



R. Kurnia, P. Turnip and E. van Groesen

Abstract For simulating phase-resolved waves in large coastal and oceanic areas, as well as in confined coastal areas and ports, efficient, stable and accurate Boussinesq type of equations for irrotational flows are much desired. Results can also be used as input for CFD calculations on smaller domains when viscous and vortical effects need to be included. In this contribution, we present examples of recent results using the AB (Analytic Boussinesq) model that has been developed based on consistent modelling of the Hamiltonian formulation of free surface waves. The pseudo-spectral AB code with various order of nonlinearity can deal with breaking waves and with spatial inhomogeneities such as bathymetry and harbour walls with fully or partially reflecting walls and breakwaters. A separate Radar Module can reconstruct and predict phase-resolved waves from radar images, and a Ship Module can deal with fully coupled wave–ship–structure interactions. In this paper, we illustrate the performance of simulations for three application areas: wave tank experiments, incoming waves in a harbour with deep access channel, and extreme, freak waves in Draupner seas as introduced in van Groesen et al., OEME 2017.

Keywords Hamiltonian Boussinesq wave modelling · Harbour waves
Freak waves · Wavetank simulations · Analytic Boussinesq model

1 Introduction

In this paper, we show the performance of the Analytic Boussinesq (AB) code that has been designed to be applicable for various ocean and coastal applications. The implementation is relatively straightforward, but the underlying modelling uses in an efficient way the most compact description of waves, which is the Hamiltonian

R. Kurnia · P. Turnip · E. van Groesen (✉)
LabMath-Indonesia, Bandung, Indonesia
e-mail: e.w.c.vangroesen@utwente.nl; groesen@labmath-indonesia.org

R. Kurnia · E. van Groesen
University of Twente, Enschede, The Netherlands

© Springer Nature Singapore Pte Ltd. 2019
K. Murali et al. (eds.), *Proceedings of the Fourth International Conference in Ocean Engineering (ICOE2018)*, Lecture Notes in Civil Engineering 23,
https://doi.org/10.1007/978-981-13-3134-3_16

formulation of Zakharov [1] and Broer [2]. They discovered that the water wave problem, i.e. the irrotational flow of a layer of incompressible fluid with a pressure-free surface, can be described as a Hamiltonian system. This is a generalization of systems with a finite degree of freedom in Classical Mechanics, to the infinite dimensional system for water waves. Using only the elevation η and the potential ϕ at the free surface, the total energy serves as the Hamiltonian. Then the generalization of the classical description is the compact formulation of the exact continuity (mass conservation) and the Bernoulli equation at the surface. The main challenge for practical applications is to express the kinetic energy explicitly in terms of the canonical variables η and ϕ . Any approximation of this energy will retain the conservation of the approximated total energy, which, when positive definite, also implies a stability property. These are two properties that in other Boussinesq equations that do not start with the Hamiltonian formulation may get lost, or may be difficult to prove, although any Boussinesq model will give the computational benefit of the dimension reduction.

The AB equation is an example of a so-called higher-order spectral method, initiated in [3]. The kinetic energy is calculated using truncations of the nonlinear Airy profiles in which the total depth is used, which leads to the need to use Fourier integral operators. In Kurnia and van Groesen [4], approximations up to fifth order are given. Extensions include a breaking scenario, and various localization methods to deal with partially or fully reflective walls [5]. The performance of the wave code has been tested for nearly 100 different study cases for which theoretical results or measurements were available. Applications run from tsunami simulations, wave tank applications, run-up on shores, bores, to waves in harbours with an access channel and freak waves in the North Sea.

In recent times, we developed a radar module with which phase-resolved waves can be reconstructed and predicted some 1–2 min in advance, using radar images of standard ship X-band radars. For high waves and waves above bathymetry, the AB software is used. A fully dynamic, Hamiltonian, implementation for coupled wave—ship interactions is in development, for ship—ship and ship-structure interactions.

In Sect. 2 a short description of the AB model is given, followed by an illustration of three-wave study cases. Discussion and conclusions finish the paper.

2 AB Model and Implementation

In this section, we briefly describe the governing equation of the AB model and some aspects of the numerical implementation.

2.1 Hamiltonian Structure

The basic dynamics is described in the canonical variables η , the surface elevation, and ϕ , the surface potential, as

$$\partial_t \eta = \delta_\phi H(\phi, \eta) \text{ and } \partial_t \phi = -\delta_\eta H(\phi, \eta) + S$$

The first equation is the continuity equation, and the second one the momentum equation. Here S is a collection of additional source terms for breaking and wave influxing and absorption described in the next subsections. For $S = 0$ the equations are Hamilton equations. The notation $\delta_\phi H$ and $\delta_\eta H$ denotes the variational derivatives with respect to the canonical variables of the Hamiltonian H . This is the total energy, sum of potential and kinetic energy K , written for notational convenience for one horizontal direction as

$$H(\phi, \eta) = 1/2 \int g\eta^2 dx + K(\phi, \eta).$$

The kinetic energy, the integral over the fluid domain of half the squared velocity, has to be considered as functional of η and of the surface potential of the internal irrotational fluid, which can only be achieved in an approximate way. In the AB model, this is explicitly done for equations up to fifth order [4].

Using such approximations, the fact that the dynamics is only for variables in the horizontal directions, without the need to solve the interior flow, makes these equations to be of Boussinesq type. The Hamiltonian structure guarantees that the total energy is conserved, and using positive definite approximations an inherent stability is achieved.

2.2 Breaking

In many practical cases, one has to deal with breaking waves. In the AB equations, breaking is modelled as a sink term in the momentum equation that reduces the energy while leaving the horizontal momentum constant. For the energy dissipation, a variant of Kennedy's eddy-viscosity model [6] is used, extended [4] to be applicable for exact dispersion. For the initiation, a kinematic breaking criterion is used, the quotient of fluid particle velocity in a crest and the crest speed. Values for this quotient are in the interval (0.7, 1) depending somewhat on the type of waves, but a deterministic method to determine this value is not yet available.

2.3 *Wave Generation and Boundary Damping Zones*

Most often, waves are generated by influx from a point or from a line; this influx method uses a source in the momentum equation that is related to the desired elevation at each position multiplied by a suitable directed acceleration [7].

Waves can also be generated from specified initial field values at an initial time over the entire simulation domain. To compensate for outflow in the simulation domain, in Sect. 3.3 we use data-assimilated influx, for which repeatedly known field data in a subdomain (instead of from a line) are merged with waves from an ongoing simulation in the complementary remaining domain [8].

Waves propagating towards outflow boundaries of the simulation domain are damped in small damping zones to prevent artificial reflection.

2.4 *Spectral Implementation*

Spectral implementations are known to be very efficient and relatively simple to implement for linear equations if spatial inhomogeneities are absent. Nonlinear terms require generalizations to spatially dependent Fourier integral operators. Slowly varying spatial changes can be dealt with in quasi-homogeneous ways, but for nonlinear terms, and when walls or partially reflecting breakwaters are present, sharp transitions may lead to Gibbs' phenomena. These problems have been overcome in the Fourier integral operators which may include step functions; retaining the (skew-) symmetry properties of the operators in the Hamiltonian is then of most importance to get the correct operators in the dynamic equations, see [4, 5].

3 *Illustration of Wave Simulations*

In this section, we illustrate the performance of the AB model outlined above for three different coastal and engineering applications.

3.1 *Wave Tank Simulations*

Most experiments in wave tanks aim to test ship behaviour in well-controlled circumstances. Then accurate generation of the desired waves is needed to obtain the correct positioning of all nonlinearly interacting wave phases and amplitudes at the position of the ship. This is illustrated here for an experiment executed at the wave tank of the Technical University of Delft [9, 10]. The tank is 142 m long, 4.22 m wide with water level of 2.13 m. Generated at one side by a single piston-type flap, the waves

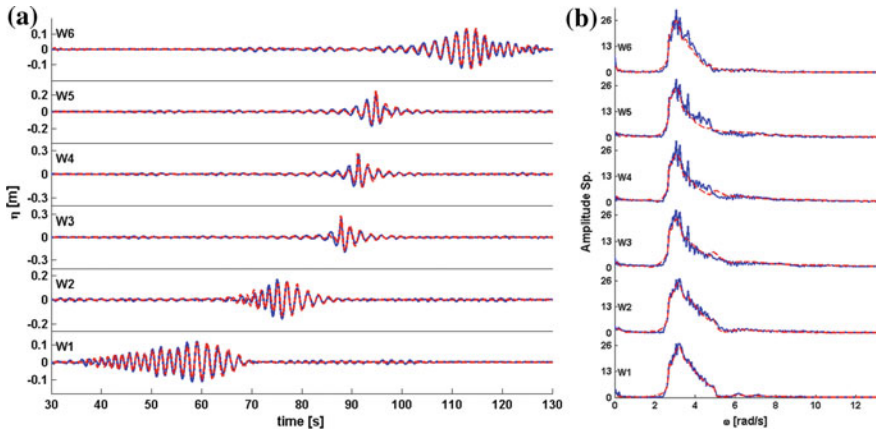


Fig. 1 Comparison of wave elevations (a) and the corresponding spectra (b) at wave probes W1–W6 between a-priori simulation (red, dashed line) and measurement (blue, solid line)

are absorbed at the other side at an artificial beach. Wave elevation measurements are located at $W1 = 10.31$ m, $W2 = 40.57$ m, $W3 = 60.83$ m, $W4 = 65.57$ m, $W5 = 70.31$ m and $W6 = 100.57$ m distance from the wave maker.

By way of example, an experimental result, identified as TUD1403Foc6, is investigated here to show the quality of the generation in the tank of an a priori given (simulated) wave field in the basin, followed by an a posteriori reconstruction of the actually generated waves using the elevation at a first measurement point as influx for a simulation.

The case to be considered is a focussing breaking wave group with peak period $T_p = 1.89$ s, peak wavelength $\lambda_p = 5.52$ m and focused at position W4. Figure 1 shows (red, dashed line) the simulation result of a priori designed wave elevations and the corresponding spectra at the measurement positions and (blue, solid line) the elevation and the corresponding spectra of the actually generated wave. The, rather small, discrepancies are mainly due to inaccuracies to translate the designed wave elevation at the wave maker position to the flap motions. This is confirmed by using as influx for a second simulation the actual laboratory elevation at the measurement position W1, and comparing the experimental result in Fig. 2 with the new simulations that show better agreement between the measurement and the simulation.

3.2 Harbour Simulations

Simulations of harbour waves have to deal with the presence of walls, partially reflecting breakwaters, bathymetric changes and possibly bottom friction. A particularly difficult case for which accurate measurements have been performed at Deltares [11] is illustrated here. The lay-out and bathymetry of the harbour with access channel of

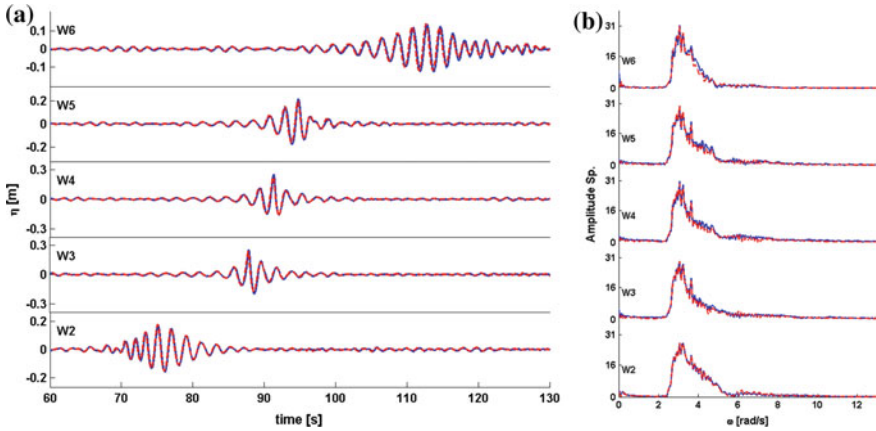


Fig. 2 Same as in Fig. 1 but now for comparison between a-posteriori simulation (red, dashed line) and the measurement (blue, solid line)

21.3 m depth in real scale is shown in Fig. 3a; the outer boundaries at the east and west sides are hard walls. Waves with a designed spectrum with 20° spreading are influxed to the North at a depth of 21.3 m from the south, west of the access channel. Immediately after generation, the waves enter the shallower part of the western harbour over a slope 1:10 till 11 m depth. The sides of the access channel have slopes of 1:5. The directional spreading of the waves cause a variety of waves in the western part. Direction and wavelength of each individual wave determine, according to Snell’s law, whether it reflects at the access channel or will refract and cross the channel to end up in the shallower eastern part of the harbour. Measurements of wave conditions at positions indicated in Fig. 3a with resistant type (WHM) and directional type (GRSM) gauges are compared with simulations. In [12, 13] results for simulations with SWASH and MIKE BW show large deviations of significant wave height, with bias of -23.6% and -27.1% respectively and average deviations of 6.6% and 9.6% respectively for the case of nonbreaking waves (T01) with $H_s = 3$ m, $T_p = 9.43$ s. Simulations with the AB code performed better for the same case, namely bias of -4.3% and deviation 2.8% . Also breaking waves, simulated only with AB, showed good results [14].

Here, we will show results for test case T02 with $H_s = 3.85$ m, $T_p = 11.90$ s and an input spectrum as shown in Fig. 3b, c. Simulations are done using the AB2 code (accurate up to and including second order). The results of the significant wave height show a bias of 0.4% and an average deviation of 4.3% . Figure 4a shows the spatial distribution of the significant heights with the errors of simulation with respect to measurement, shown in percentage at the wave gauge positions. The relatively small errors indicate that the simulation is able to reconstruct the wave conditions in the wave-ward side of the channel, inside the channel and in the lee-ward side of the channel, with highest errors appearing at WHM01 and WHM07. From the H_s plot, it can be seen that most of the wave energy is concentrated along the wave-ward side

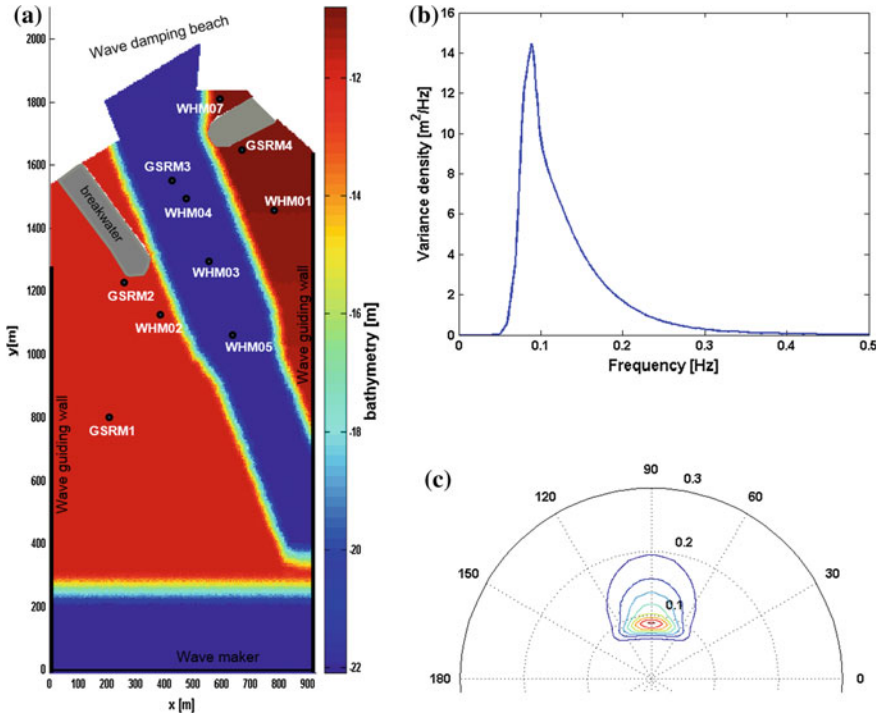


Fig. 3 Shown are **a** the physical model setup of the harbour with the access channel making a complicated bathymetry as indicated by the colouring according to the colour bar, **b** the one-dimensional input spectrum and **c** the two-dimensional wave spectrum for the generation of waves for test case T02 with contours lines enclosing various levels of energy

of the channel that leads to wave breaking in front of the breakwater, see Fig. 4b for a snapshot with wave breaking.

3.3 Freak Waves in Draupner Seas

Scientific interest in high seas with abundant appearance of freak waves let us design and investigate ‘Draupner seas’ that resemble the sea at the moment that the well-known Draupner wave of 18 m crest height was measured from the Draupner platform on 1 January 1995 in the north sea. Using new meteorological insights [15], the very wide spectrum has long wave lobes at the side as shown in Fig. 5 in which a rotation has been applied to have the main wave propagation from North to South.

In [8] we simulated such seas in a large area, using data-assimilated influx of linear waves along a circular arc, and investigated details in a much smaller rectangular area of 15 km² where nonlinear effects, including four-wave interaction, have

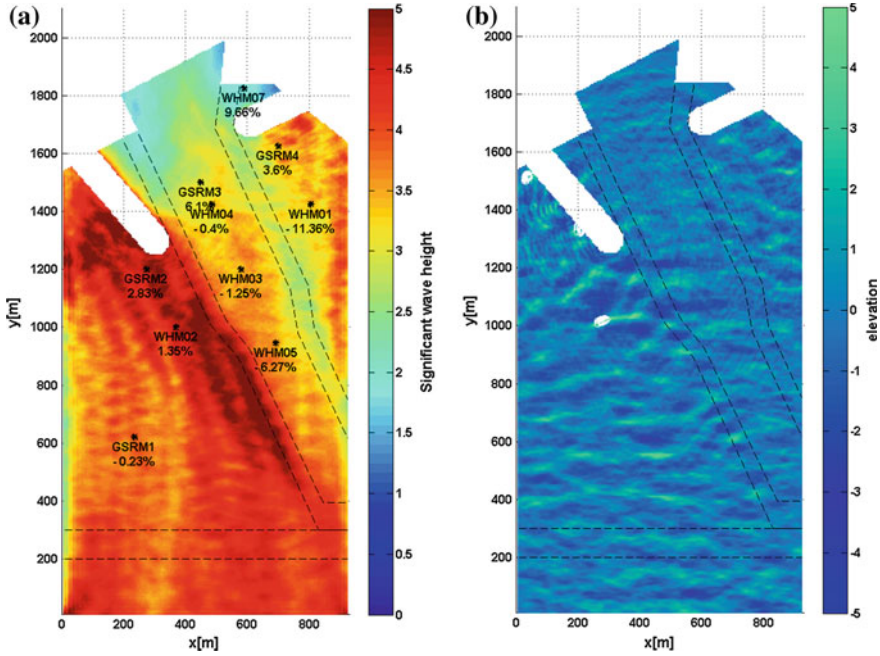


Fig. 4 **a** Shown are the density plot of the spatially varying significant wave height. The error of the calculations compared to the measurement data are indicated at the wave gauge positions. **b** Snapshot of the elevation at $t = 1340$ s; breaking waves are indicated by white foam (circles)

been developed. Here we show results of one of the in total 40 seas that have been simulated, identified as sea 17 m4.

This sea has $H_s = 12.1$ m and $T_p = 15$ s, and the largest crest height in the simulation of 200 waves for this sea was found to be a freak wave of 20 m crest height, more than $1.6 H_s$. From statistical results [8], the probability of such a crest height in this sea is as high as $1.85 \times 10^{-9}/m^2$ per period, i.e. can be expected on an area of 1 km^2 almost once every 2 h. An impression of the sea elevation at the time of the freak event is shown in a neighbourhood of the freak wave in Fig. 6, and in the North–South direction at a transect through the freak position in Fig. 7. The time trace of the elevation at the freak position is given in Fig. 8.

4 Discussion and Conclusions

The illustrations for various applications given in Sect. 3 show that accurate wave simulations are possible with the AB code. The a priori design of desired waves in a wave tank can be used to improve if needed, the software to steer the wave flap. The a posteriori simulation of generated waves can, for instance, be used to take the

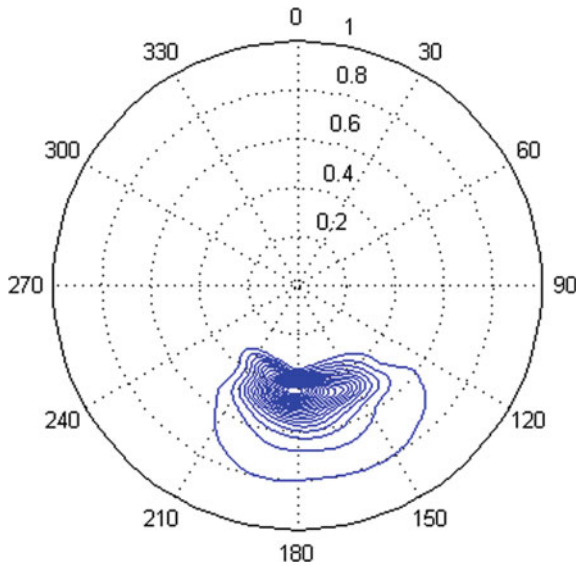


Fig. 5 The 2D spectrum as shown in [8] based on [16]

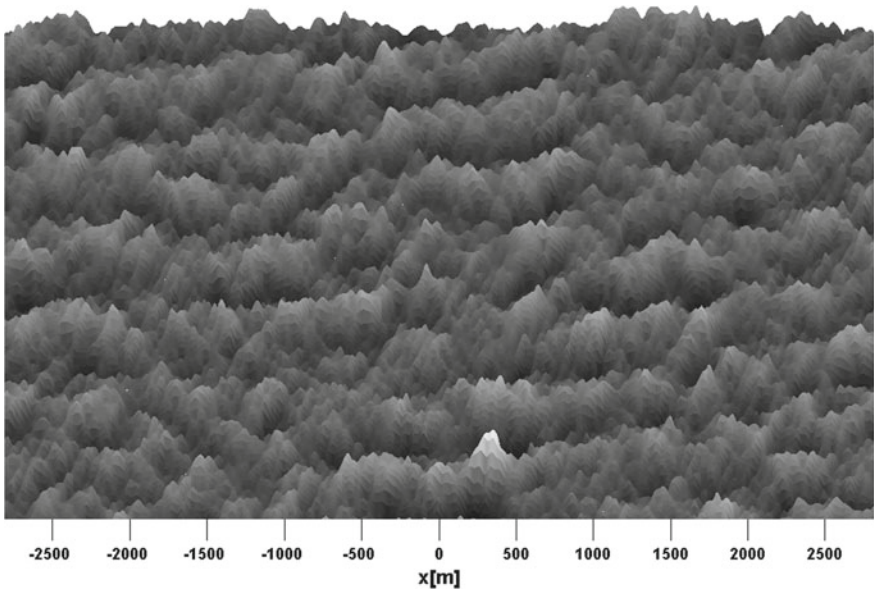


Fig. 6 Plot of the sea state at time 2048.7 s looking from south (bottom) to north over the whole observation area. The highest crest, with *white cap*, is positioned at $x = 350.7$ m, $y = 456$ m

quantitative results as input in a much smaller area for more precise CFD calculations on structures in that area. Simulation of waves in harbours are of profound importance

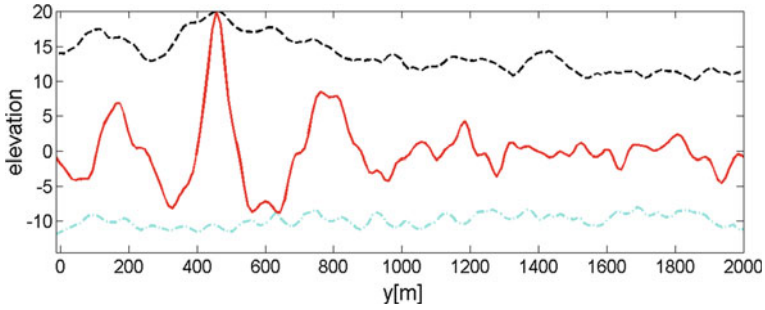


Fig. 7 Plot of the elevation profile (red, solid line) at a cross-section along the y-axis at $x = 350.7$ m at time of the freak wave event. The maximum and minimal temporal elevation is shown by the dashed line (black) and by dashed-dot line (cyan)

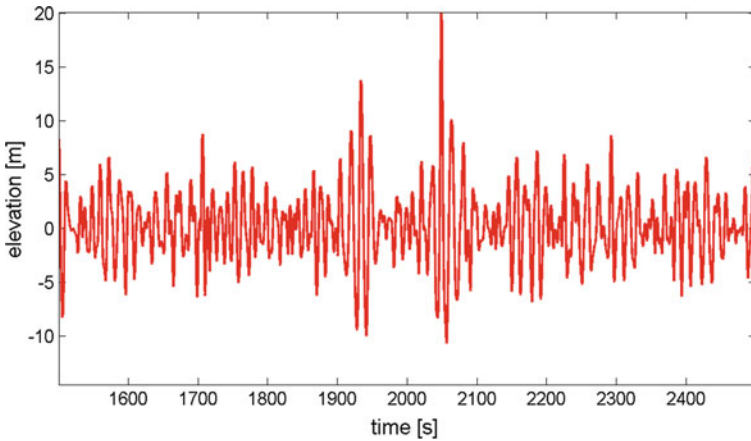


Fig. 8 Plot of the elevation time trace at the freak wave position, $x = 350.7$ m, $y = 456$ m

for the design of harbours and are a prerequisite for simulations of motions of moored ships in an existing harbour, which may also lead to more optimal performance for loading operations. Simulations of high waves in seas and oceans that include four-wave interactions are of interest to increase our knowledge about the various physical aspects that dominate the appearance and the 2D patterns of complicated wave crests.

The wave software, under the name HAWASSI, see www.hawassi.labmath-indonesia.org, is freely available after registration for university thesis work, and arrangements can be tailor-made for other purposes. A Radar Module is under development to predict waves, including freak waves as in Sect. 3.3, ahead of their appearance [16, 17]. A ship module for fully coupled wave–ship–structure interactions are being developed for future releases.

Acknowledgements We are grateful for the use of data of measurements at TUD and Deltares in The Netherlands, and for information about the spectrum used for the Draupner seas from the European Centre for Medium-Range Weather Forecasts, Reading, UK. Riam Badriana contributed to simulations for the access channel. R.K. was partly funded by the Netherlands Organization for Scientific Research NWO, Technical Science Division STW Project 11642.

References

1. Zakharov VE (1968) Stability of periodic waves of finite amplitude on the surface of a deep fluid. *J Appl Mech Tech Phys* 9:190–194
2. Broer LJF (1974) On the Hamiltonian theory of surface waves. *Appl Sci Res* 29:430–446
3. Dommervuth DG, Yue DKP (1987) A high-order spectral method for the study of nonlinear gravity waves. *J Fluid Mech* 184:267
4. Kurnia R, van Groesen E (2014) High order Hamiltonian water wave models with wave-breaking mechanism. *Coast Eng* 93:55–70
5. Kurnia R, van Groesen E (2017) Localization for spatial-spectral implementations of 1D analytic Boussinesq equations. *Wave Motion* 72:113–132
6. Kennedy AB, Chen Q, Kirby JT, Dalrymple RA (2000) Boussinesq modeling of wave transformation, breaking, and runup. *J Waterw Port Coast Ocean Eng* 126:39–47
7. Lie SL, Adytia D, van Groesen E (2014) Embedded wave generation for dispersive surface wave models. *Ocean Eng* 80:73–83
8. Van Groesen E, Turnip P, Kurnia R (2017) High waves in Draupner seas, part 1: numerical simulations and characterization of the seas. *J Ocean Eng Mar Energy* 3:233–245
9. Kurnia R, van den Munckhov T, Poot CP, Naaijen P, Huijsmans RHM, van Groesen E Simulations for design and reconstruction of breaking waves in a wavetank. In: ASME 34th international conference on ocean, offshore and arctic engineering (OMAE). St. John's, NL, Canada, ASME. OMAE2015–41633
10. Kurnia R, van Groesen E: Design of wave breaking experiments and A-Posteriori Simulations (Memorandum Department of Applied Mathematics; No. 2042), Enschede, University of Twente (2015)
11. Van der Werf IM, Hofland B (2012) Internal report. Deltares
12. Dusseljee D, Klopman G, van Vledder G, Riezebos HJ (2014) Impact of harbor navigation channels on waves: a numerical modelling guideline. *Coast Eng Proc* 1(34):58
13. Monteban D (2016) Numerical modelling of wave agitation in ports and access channels. Master Thesis, TU Delft
14. Kurnia R, Badriana M, van Groesen E (2018) Hamiltonian Boussinesq simulations for waves entering a harbour with access channel. *J Waterw Port Coast Ocean Eng* 144(2):04017047
15. Cavaleri L, Benetazzo A, Barbariol F, Bidlot J-R, Janssen PAEM (2017) The Draupner event: the large wave and the emerging view. *Bull Am Meteor Soc* 98:729–735
16. Wijaya AP, Naaijen P, Andonowati, van Groesen E (2015) Reconstruction and future prediction of the sea surface from radar observations. *Ocean Eng* 106:261–270
17. Van Groesen E, Wijaya AP (2017) High waves in Draupner seas, part 2: observation and prediction from synthetic radar images. *J Ocean Eng Mar Energy* 3:325–332